Initial Human PET Imaging Studies with the Dopamine Transporter Ligand ^{18}F-FECNT

Margaret R. Davis, MD[1,2]; John R. Votaw, PhD[1,3]; J. Douglas Bremner, MD[1,3,4]; Michael G. Byas-Smith, MD[5]; Tracy L. Faber, PhD[1,3]; Ronald J. Voll, PhD[1,3]; John M. Hoffman, MD[6]; Scott T. Grafton, MD[7]; Clinton D. Kilts, PhD[4]; and Mark M. Goodman, PhD [1,3,4]

[1]PET Center, Emory University, Atlanta, Georgia; [2]Department of Neurology, Emory University, Atlanta, Georgia; [3]Department of Radiology, Emory University, Atlanta, Georgia; [4]Department of Psychiatry and Behavioral Sciences, Emory University, Atlanta, Georgia; [5]Department of Anesthesiology, Emory University, Atlanta, Georgia; [6]Biomedical Imaging Program, National Cancer Institute, National Institutes of Health, Bethesda, Maryland; and [7]Center for Cognitive Neuroscience, Dartmouth College, Hanover, New Hampshire

The aim of this study was to do an initial assessment of the usefulness of 2β-carbomethoxy-3β-(4-chlorophenyl)-8-(2-^{18}F-fluoroethyl)nortropane (^{18}F-FECNT) PET scanning in determining in vivo brain dopamine transporter (DAT) density in healthy humans and subjects with Parkinson's disease (PD). **Methods:** We investigated 6 neurologically healthy subjects and 5 PD patients: 2 with mild unilateral disease, 1 with mild-to-moderate bilateral disease, and 2 with moderately severe bilateral disease. The healthy subjects underwent a 3-h PET scan (26 frames) and the PD subjects underwent a 2-h PET scan (23 frames) while ^{18}F-FECNT was being injected over the first 5 min of the scan. Arterial blood samples were taken throughout scanning for well-counter and metabolite analysis to determine the presence of possible active metabolites. The scans were reconstructed; then we placed spheric regions of interest in the caudate nuclei, putamena, thalami, brain stem, cerebellum, and occipital cortex of each subject. The radioactivity level in each region was calculated for each frame of a subject's PET scan. Then we calculated target tissue-to-cerebellum ratios for each time frame. **Results:** The analysis of arterial blood samples revealed that metabolism of the tracer was rapid. The ether-extractable component of the arterial input was >98% pure ^{18}F-FECNT. The caudate nucleus and putamen exhibited the highest uptake and prolonged retention of the radioligand. They both attained maximum uptake at ~90 min, with the healthy subjects' average caudate- and putamen-to-cerebellum ratios (±SD) at that time being 9.0 ± 1.2 and 7.8 ± 0.7, respectively. The maximal caudate-to-cerebellum ratios for the healthy subjects ranged from 7.6 to 10.5 and their maximal putamen-to-cerebellum ratios ranged from 7.1 to 9.3. The 2 early-stage, unilateral PD patients had, at 90 min, an average right caudate-to-cerebellum ratio of 5.3 ± 1.1 and a left ratio of 5.9 ± 0.7 and an average right putamen-to cerebellum ratio of 2.8 ± 0.1 and a left ratio of 3.0 ± 0.6. The late-stage PD patients had, at 90 min, an average right caudate-to-cerebellum ratio of 3.7 ± 0.4 and a left ratio of 3.9 ± 0 and an average right putamen-to cerebellum ratio of 1.8 ± 0.1 and a left ratio of 1.8 ± 0. **Conclusion:** These results indicate that ^{18}F-FECNT is an excellent candidate radioligand for in vivo imaging of the DAT system in humans. It has a much higher affinity for DAT than for the serotonin transporter and yields the highest peak striatum-to-cerebellum ratios and has among the most favorable kinetics of ^{18}F-radiolabeled DAT ligands. Having picked up presymptomatic changes in the hemisphere opposite the unaffected side of the body in our early-stage (unilateral) PD patients, it appears that, like other DAT radioligands, it may be able to identify presymptomatic PD.

Key Words: dopamine transporter; PET; 2β-carbomethoxy-3β-(4-chlorophenyl)-8-(2-^{18}F-fluoroethyl)nortropane; Parkinson's disease

J Nucl Med 2003; 44:855–861

Many disease states, including Parkinson's disease (PD), schizophrenia, attention deficit disorder, and drug abuse, are attributed to abnormalities within the brain's dopamine system. The dopamine transporter (DAT) protein is critical to the regulation of synaptic concentration of dopamine, and thus dopamine neurotransmission, in the brain. When combined with PET or SPECT, ligands binding specifically to the DAT are potentially useful as in vivo imaging tools for studying these various illnesses and evaluating the degrees of success of their treatments. DAT density is also a marker of the integrity and number of presynaptic terminals of dopamine-producing neurons. PD dramatically decreases the number of presynaptic striatal dopaminergic neurons (hence, DAT density) and thus can be assessed using these imaging agents. Several radioligands have been used to study and quantify brain DAT. A class of cocaine analogs known as WIN compounds (*1*,*2*) have been synthesized and used as radiopharmaceuticals for in vivo imaging of the DAT with both PET and SPECT. 2β-Carbomethoxy-3β-(4-^{123}I-iodophenyl)tropane (^{123}I-β-CIT) has been used as a SPECT imaging agent for evaluation of the DAT (*3*–*6*). Several studies document the loss of

Received Sep. 9, 2002; revision accepted Jan. 21, 2003.

For correspondence or reprints contact: Mark M. Goodman, PhD, Department of Radiology, Emory University Hospital, 1364 Clifton Rd., N.E., Atlanta, GA 30322.

E-mail: mgoodma@emory.edu

striatal uptake of ^{123}I-β-CIT in PD (*6–9*). A commonly used alternative imaging method is to assess presynaptic dopaminergic function with the radiolabeled catecholamine precursor fluoro-L-DOPA (F-DOPA). On the basis of studies of parkinsonian rats comparing ^{14}C-L-DOPA and ^{123}I-β-CIT, it was proposed that ^{123}I-β-CIT might better define the severity and rate of progression of PD than the ligand F-DOPA (*10*).

Because of the higher spatial resolution (4–6 mm) currently available with PET as compared with multihead SPECT (8–10 mm) imaging systems, PET is generally considered the more informative imaging modality for the quantitative measurement of the in vivo density of neurotransmitter transporters and receptors in humans. ^{18}F is the most attractive radionuclide for radiolabeling PET ligands because its 110-min half-life allows sufficient time for synthesis and incorporation into the tracer molecule and for purification of a final product suitable for human administration. Additionally, ^{18}F can be prepared as fluoride ion in becquerel quantities for incorporation into the tracer molecule routinely in high attainable (typically >37 GBq/μmol) specific activity by no-carrier added nucleophilic substitution reactions. ^{18}F is also one of the lowest energy positron emitters (0.635 MeV; 2.4-mm positron range), which affords the highest resolution images. Finally, the half-life of ^{18}F permits a detailed characterization of the entry and regional uptake of the radioligand in the brain and facilitates the analysis of the presence of radiolabeled metabolites. ^{18}F-Labeled DAT ligands that have been developed over the past few years include *N*-3-^{18}F-fluoropropyl-2β-carbomethoxy-3β-(4-iodophenyl)nortropane (^{18}F-FPCIT) (*11*), 2β-carbomethoxy-3β-(4-^{18}F-fluorophenyl)tropane (^{18}F-CFT) (*12*), 2β-carbomethoxy-3β-(4-chlorophenyl)-8-(3-^{18}F-fluoropropyl)nortropane (^{18}F-FPCT) (*13*), ^{18}F-(+)-*N*-(4-fluorobenzyl)-2β-propanoyl-3β-(4-chlorophenyl)tropane (^{18}F-FCT) (*14*), 2′-^{18}F-fluoroethyl-(1*R*-2-exo-3-exo)-8-methyl-3-(4-chlorophenyl)-8-azabicyclo[3.2.1]octane-2-carboxylate (^{18}F-FECT) (*15*), 2′-^{18}F-fluoroethyl-(1*R*-2-exo-3-exo)-8-methyl-3-(4-methylphenyl)-8-azabicyclo[3.2.1]octane-2-carboxylate (^{18}F-FETT) (*15*), 2β-(*R*,*S*)-carbo-1-^{18}F-fluoro-2-propoxy-3β-(4-chlorophenyl)tropane (^{18}F-FIPCT) (*16*), and *N*-3-^{18}F-fluoropropyl-2β-carbomethoxy-3β-(4′-methylphenyl)nortropane (^{18}F-FPCMT) (*17*).

We have previously described the synthesis of ^{18}F-2β-carbomethoxy-3β-(4-substituted-phenyl)nortropanes with different *N*-fluoroalkyl substituents as DAT, PET imaging agents (*13,16,18*). Our results indicate that 2β-carbomethoxy-3β-(4-chlorophenyl)-8-(2-^{18}F-fluoroethyl)nortropane (^{18}F-FECNT) has the lowest nonspecific binding and most favorable DAT binding kinetics (*17*). In previous experiments with cells transfected with human (h) DAT, serotonin transporter (SERT), and norepinephrine transporter (NET) complementary DNA, ^{18}F-FECNT was shown to have 25-fold greater affinity for hDAT than for hSERT and 156-fold greater affinity for hDAT than for hNET (*18*). Figure 1 shows the chemical structure of ^{18}F-FECNT. Dosimetry estimates for ^{18}F-FECNT in humans have been published (*19*).

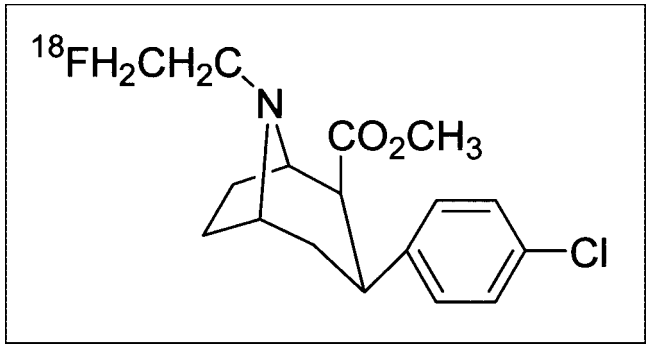

FIGURE 1. Chemical structure of ^{18}F-FECNT.

^{18}F-FECNT has proven to be a useful tool for in vivo estimation of striatal DAT occupancy in nonhuman primates. A PET study of ^{18}F-FECNT displacement with cocaine showed that intravenous cocaine doses of 0.1 and 1.0 mg/kg, both of which have significant behavioral reinforcing effects in intravenous self-administration studies in nonhuman primates, occupy 53% ± 5% and 87% ± 5% (*20*) of DAT, respectively. This is consistent with data in ^{11}C-cocaine PET studies of cocaine-related striatal DAT occupancy in baboons (*21*) and humans (*22*). Another study used ^{18}F-FECNT displacement to determine the level of DAT occupancy associated with maximum reinforcing effects of RTI-113, a cocaine analog that serves as a selective, high-affinity dopamine uptake inhibitor (*23*). Finally, a recent study discusses the use of a generalized tissue reference model for ^{18}F-FECNT in multiphase experiments, where quasiequilibrium is not reached in at least 1 phase of the experiment (*24*).

In this article we describe our initial results using ^{18}F-FECNT as a tool for assessing in vivo brain DAT density in healthy human volunteers and 2 patients with PD. Representative images, typical time–activity curves, and target tissue-to-cerebellum ratios for the healthy individuals and the PD patients are presented. We also describe the metabolism of ^{18}F-FECNT in humans.

MATERIALS AND METHODS

Subjects

Six neurologically healthy subjects and 5 PD patients participated in this study. The healthy subjects included 3 men and 3 women with a mean age (±SD) of 30 ± 10 y). The PD patients included 3 women and 2 men. Two of the patients were hemi-PD and had modified Hoehn and Yahr (H&Y) (*25*) scores of 1.5, 1 patient had moderate bilateral disease and an H&Y score of 2.5, and 2 patients had moderately severe disease and H&Y scores of 4. In the healthy volunteers, absence of past or present psychiatric and neurologic disorders was confirmed by history, review of systems, and neurologic examination. In particular, none of these subjects had a history of drug abuse, schizophrenia, or movement disorders. None of these subjects had taken any centrally acting drugs (prescription or nonprescription), except caffeine, for at least 2 mo before being imaged. The PD patients were allowed to continue taking their routine anti-PD medications on the day of the

scan because several investigators have shown that such medications do not interfere with DAT imaging (*26–28*). The study was approved by the Human Investigations Committee of Emory University, and written informed consent was obtained from each subject after the study had been thoroughly explained and before participation in the study.

Radiochemistry

^{18}F-FECNT's preparation has been previously reported (*18*). In 10 subjects, following the reported methodology, the radiochemical yield of the desired product was 16.5% ± 5.3% and its radiochemical purity was 99.8% ± 0.4%. The average specific activity for the radiochemical yield at the end of bombardment was 38 ± 45 GBq/μmol and at the time of injection was 6 ± 8 GBq/μmol. See Table 1 for a breakdown by individual subjects.

PET

Quantitative brain PET images were acquired using an ECAT 921 EXACT scanner (Siemens/CTI) (*29*). The scanner has an axial field of view of 16.2 cm. All subjects were fasted for 4 h before scanning to minimize spikes of neutral amino acid levels in their plasma. They were placed into the tomograph gantry and their heads were immobilized using a thermoplastic facemask (TruScan). Before injection of the radiotracer, a 15-min transmission scan was obtained using a ^{68}Ge source for attenuation correction of the emission data.

^{18}F-FECNT was delivered through an intravenous line over a 5-min period. An average of 175.1 ± 41.3 MBq of radioligand were injected. The healthy subjects were scanned in 3-dimensional mode for 180 min using 26 frames of increasing duration (10 × 30 s, 5 × 1 min, 5 × 10 min, 6 × 20 min). The PD patients were scanned just as the healthy subjects, except that the last 3 frames were eliminated to give a total scan time of 120 min. Images were reconstructed with a Hahn filter (cutoff frequency, 1 cycle/cm) giving an approximate isotropic resolution of 8.0-mm full width at half maximum.

Arterial blood sampling was performed in 5 of the healthy volunteers and 2 of the PD patients to permit metabolite analysis. In these subjects the radial artery was catheterized before immobilization of their head and after the performance of the Allen test and subcutaneous injection of lidocaine. Arterial sampling involved taking twenty-two 1.5-mL samples for well-counter analysis of radioactivity (1 sample every 30 s for the first 8 min, followed by samples at 10, 20, 30, 60, 120, and 180 min) and seven 5.0-mL samples (collected at 2, 6, 10, 20, 60, 120, and 180 min) for metabolite analysis. Metabolite analysis was done by methodology described previously (*18*).

Data Analysis

Images were initially realigned using a method designed by Lin et al. to correct for subject movement during F-DOPA imaging (*30*) that was adapted to FECNT imaging. The last 4 frames of the dynamic image set were summed to form a DAT (late phase) image, and the first 14 images were summed to form a flow image. Spheric regions of interest (ROIs) were drawn on the 2 summed images and then applied to the dynamic image set. The caudate nucleus and putamen ROIs were placed on the DAT summed image. Two nonoverlapping spheres measuring 1.0 cm in diameter (to the nearest pixel) were centered in each caudate nucleus in 2 nonconsecutive planes. In each of 2 nonconsecutive planes, 3 nonoverlapping spheres, each measuring 0.7 cm in diameter, were placed in each putamen. On the summed flow image, two 1.75-cm-diameter nonoverlapping spheres were placed in each hemisphere of the cerebellum and one 3.0-cm-diameter sphere was placed in each hemisphere of the occipital cortex. Also, in 2 nonconsecutive planes, 1.0-cm-diameter spheres were placed in the brain stem and each thalamus. Upon applying the ROIs to the dynamic image set, time–activity curves decay corrected to the time of injection were generated.

RESULTS

Analysis of arterial blood samples revealed that metabolism of the tracer was rapid, with ~40% of the radioactivity remaining in the plasma at 20 min after injection, of which 35% was the parent compound. The major metabolite of ^{18}F-FECNT in the arterial samples was a polar component.

TABLE 1
Breakdown of Radiochemistry Data

Subject no.	Radiochemical purity (%)	Radionuclide purity (%)	Radiochemical yield (%)	SA at end of bombardment (GBq/μmol)	SA at injection (GBq/μmol)
1	100	100	28	25	6
2	100	100	15	25	6
3	100	100	15	25	1
4	100	100	8.5	4	740*
5	99	100	13	122	29
6	99	100	13	122	7
H&Y 4♂	100	100	15	5	1
7†	100	100	21	12	2
8†	100	100	17	25	6
9†	100	100	19	12	3

*MBq/μmol.

†Subjects 7–9 are healthy individuals who are not discussed in this article. Data for remaining 4 PD patients were not immediately available.

SA = specific activity; H&Y 4♂ = H&Y stage 4, male PD patient.

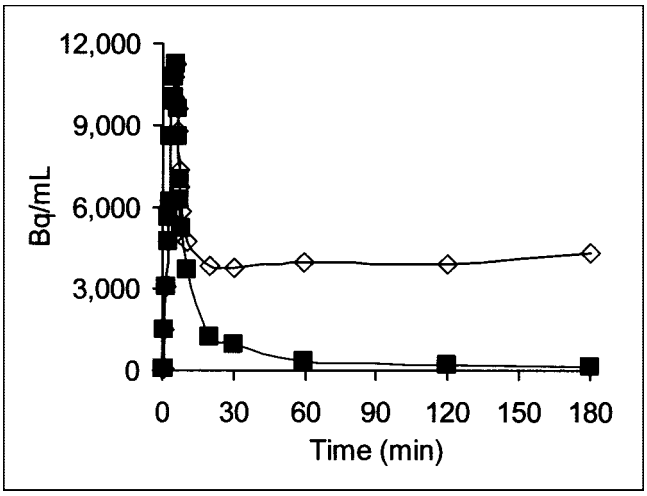

FIGURE 2. Arterial plasma time–activity curve from typical healthy subject (subject 4, Table 1) injected with 206 MBq ^{18}F-FECNT. Total arterial ^{18}F plasma activity (◇) and arterial parent ^{18}F-FECNT plasma activity (■) are shown.

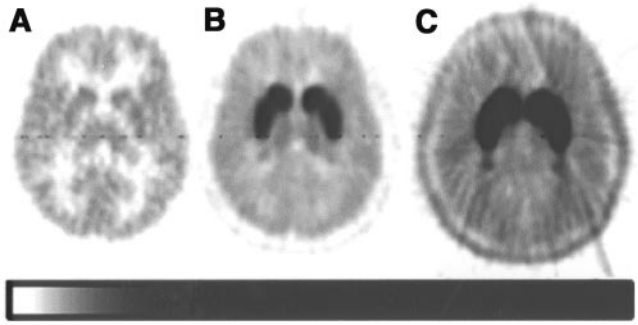

FIGURE 3. Summed early-phase (0–15 min) (A), middle-phase (16–65 min) (B), and late-phase, or DAT (66–185 min) (C) ^{18}F-FECNT PET images in typical healthy volunteer (subject 5, Table 1). Images were normalized to maximum average cerebellar uptake, yielding equal scaling. Note that color scale is not linear. Images had to be γ-corrected (with shift of γ-scale to left) so that first 2 images could be seen.

The ether-extractable component of the arterial input was >98% pure ^{18}F-FECNT. Figure 2 is a representative blood time–activity curve of a healthy volunteer.

Table 2 shows each subject's age, sex, the time at which maximum uptake was attained, and the caudate- and putamen-to-cerebellum ratios at that time. Figure 3 shows the summed ^{18}F-FECNT early-, middle-, and late-phase (DAT) images in a typical healthy volunteer. A high initial uptake of radioactivity occurs in the brain, with the cerebellum and occipital cortex exhibiting maximal activity at ~7.5–10 min after injection. The thalamus is slightly, but visibly, labeled in the early- and middle-phase images but not in the late image (Fig. 3). It reaches maximal uptake between 10 and 15 min after injection. The caudate nucleus and putamen exhibit the highest uptake and prolonged retention of the radioligand. The caudate and putamen are the only brain regions visibly labeled by ^{18}F-FECNT in the late-phase summed images (i.e., 66–185 min after injection) (Fig. 3). The caudate and putamen reach maximum total activity at ~45 min. The caudate and putamen both attain maximum specific activity at ~90 min, with the healthy subjects' average caudate- and putamen-to-cerebellum ratios at that time being 9.0 ± 1.2 and 7.8 ± 0.7, respectively. However, as is shown in Table 2, not all subjects attained maximum uptake at 90 min. The time of maximal uptake ranged from 70 to 130 min. The maximal caudate-to-cerebellum ratios for the healthy subjects ranged from 7.6 to 10.5 and their maximal putamen-to-cerebellum ratios ranged from 7.1 to 9.3. The differences in caudate- and putamen-to-cerebellum ratios are most likely attributable to the size of the region chosen and to the partial-volume effect.

Figure 4 shows representative time–activity curves from a typical healthy subject for the caudate, putamen, thalamus, occipital cortex, brain stem, and cerebellum. It is a logarith-

TABLE 2
Comparison of Healthy and PD Subjects' Demographic and PET Data

Subject no. or score	Sex	Age (y)	Time at max. total caud and put activity (min)	Time at max. SCRs (min)	Max. caud:cer	Max. put:cer
1	M	46	35	90	7.6	7.3
2	M	23	55	130	10.4	8.0
3	M	27	45	110	8.2	7.1
4	F	24	45	90	8.7	8.1
5	M	22	35	90	9.7	8.0
6	F	40	35	70	10.5	9.3
H&Y 1.5	M	65	25	90	5.0	2.7
H&Y 1.5	F	36	25	90	5.5	3.0
H&Y 2.5	F	46	25	90	4.4	2.0
H&Y 4	F	65	9.5	70	3.9	1.8
H&Y 4	M	69	15	90	3.5	1.8

Max. = maximum; caud = caudate nucleus; put = putamen; SCRs = striatum-to-cerebellum ratios; cer = cerebellum; H&Y = H&Y stage.

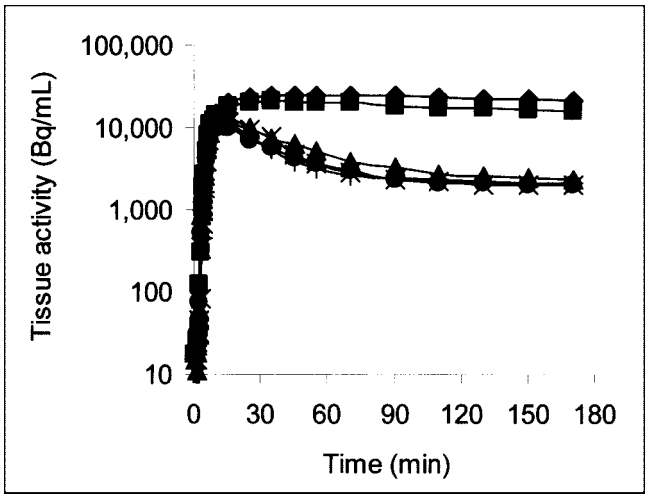

FIGURE 4. Logarithmic plot of brain tissue time–activity curve in healthy 63.4-kg male subject (subject 2, Table 1) injected with 216 MBq ^{18}F-FECNT. Brain regions represented are caudate (◆), putamen (■), thalamus (▲), brain stem (×), occipital cortex (+), and cerebellum (●).

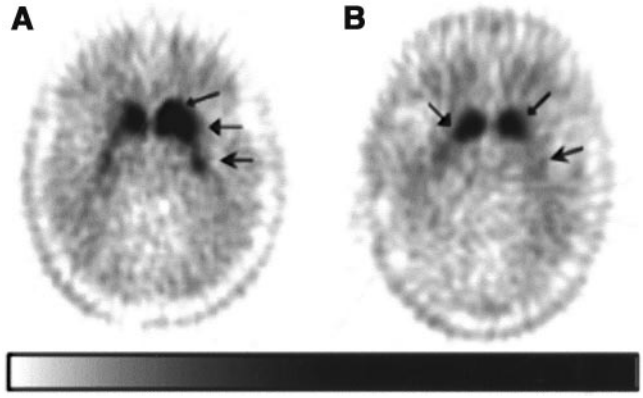

FIGURE 5. Late-phase (60 min) images of DAT ^{18}F-FECNT PET scans of H&Y stage 1.5 (A) and stage 4 (B) PD patients. Images were normalized to maximum cerebellar uptake, yielding equal scaling. Note that caudate (→) and anterior putamen (→) are still fairly intact (caudate nuclei more so than anterior putamen) in H&Y stage 1.5 subject, whereas posterior putamen (↔) are of nearly equal contrast, or deterioration, in both H&Y 1.5 and H&Y 4 subject. Also, note that color scale is not linear. Images were γ-corrected (with shift of γ-scale to left) so that they could be better seen.

mic plot of the time–activity curves of subject 2 in Table 2. Figure 4 shows that the thalamus, brain stem, occipital cortex, and cerebellum total activities peak at ~15 min after injection in this individual and then fall off rapidly, whereas the caudate and putamen activities peak at ~60 min and remain high, falling off very little. The time–activity curves for all but the thalamus reach equilibrium (i.e., become parallel to the plasma) between 90 and 110 min after injection. The thalamus appears to reach equilibrium around 130 min after injection. Table 3 shows the average target tissue-to-cerebellum ratios versus time for the healthy subjects. It shows that the caudate- and putamen-to-cerebellum ratios peak at ~90 min after injection, whereas the thalamus- and brain stem-to-cerebellum ratios peak at ~35–45 min after injection. Figure 5 shows FECNT images at 60 min after injection for 2 of the PD patients, illustrating the imaging differences between early, hemi-PD, and late-stage PD. Figure 6 compares the right and left caudate- and putamen-to-cerebellum ratios of the healthy subjects' average and the H&Y stage 1.5, 2.5, and 4 PD patients. We found that in all PD patients, the caudate-to-cerebellum ratios were much higher than the putamen-to-cerebellum ratios. In the H&Y stage 4 patients the right and left striatum-to-cerebellum ratios (SCRs) were nearly equal to each other. However, in the H&Y stage 1.5 patients, the caudate-to-cerebellum ratios were notably larger in the hemispheres of the brain opposite the unaffected sides of their bodies; the putamen-to-cerebellum ratios were much lower bilaterally, although slightly, but recognizably, larger in the hemispheres opposite the unaffected sides of their bodies. Visually, one could easily identify their unaffected sides by viewing the differences in anterior putamena uptake. The H&Y stage 2.5

TABLE 3
Average Tissue-to-Cerebellum Ratios vs. Time After ^{18}F-FECNT Injection in Healthy Subjects

Time (min)	Ratio			
	Caud:cer	Put:cer	Thal:cer	Brain stem:cer
35	5.1	4.6	1.4	1.3
90	9.0	7.8	1.3	1.1
110	8.9	7.6	1.2	1.1

Caud = caudate nucleus; cer = cerebellum; Put = putamen; Thal = thalamus.

Note that brain stem and thalamus have greater uptake than background, probably due to DAT in substantia nigra and loosely configured areas of DAT in thalamus.

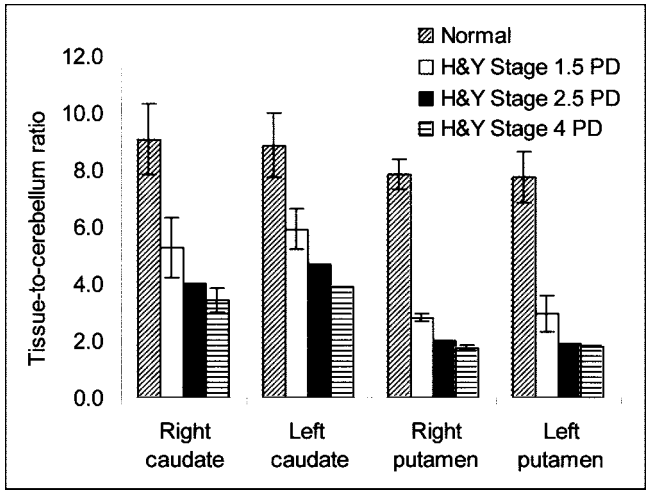

FIGURE 6. Comparison of tissue-to-cerebellum ratios at 90 min after injection of healthy subjects and PD patients.

patient's caudate-to cerebellum ratios were somewhat in between those of the hemi-PD and moderately severe PD patients, but her putamen-to-cerebellum ratios were much more significantly decreased than the hemi-PD patients, showing little difference between each other and with the ratios seen in the 2 moderately severe disease patients.

DISCUSSION

To our knowledge, this work describes the first human studies using ^{18}F-FECNT. The 3-h time–activity curves from all 6 healthy volunteers (Fig. 4 is typical) show that uptake peaks at about 90 min after injection in the striatum and then decreases. In other less DAT-rich tissues, uptake peaks between 7.5 and 15 min and then decreases. After 100 min, the uptake decreases in all tissues and the plasma at about the same rate. Thus, it appears that ^{18}F-FECNT is at or near quasiequilibrium and that the amount of irreversible binding, if any, is small. This is consistent with previous primate chase studies in which injection of β-CIT caused ^{18}F-FECNT to clear from the striatum with a half-rate of 10.4 min (*18*).

The target tissue-to-cerebellum ratios shown in Table 3 are consistent with the in vitro data using unlabeled FECNT (*18*). The ratios show that ^{18}F-FECNT has a much higher affinity for DAT than for SERT. The areas of human brain known to have the richest supply of SERT are the brain stem, containing the raphe nucleus, and the thalamus (*31*). The graphic shows that the ratios from greatest to least are caudate $>$ putamen $\gg$ thalamus $>$ brain stem.

The SCRs for ^{18}F-FECNT are the highest of the DAT-selective compounds reported in primates thus far. ^{18}F-FCT has an SCR of 2.6 (*14*) and ^{18}F-S-FIPCT has a ratio of ~2.9 (*16*). ^{18}F-FPCIT, ^{18}F-FPCT, and ^{18}F-(*R*)-FIPCT each have SCRs of ~3.5 (*11*,*13*,*16*,*32*), with $P < 0.001$ on a 2-tailed Student *t* test when comparing the SCR of ^{18}F-FPCIT with ^{18}F-FECNT. ^{18}F-CFT has an SCR of ~5.8 (*12*) compared with ^{18}F-FECNT's SCR of ~8.2 (2-tailed Student *t* test; $P < 0.001$). Also, ^{18}F-FECNT has favorable binding kinetics compared with the majority of these ligands. ^{18}F-FPCT does not reach maximal binding until 115 min (*13*) and ^{18}F-CFT does not reach maximal binding until 225 min after injection (*12*). ^{18}F-FPCIT reaches maximal binding at the same time (~90 min) (*11*) as ^{18}F-FECNT. ^{18}F-FCT and ^{18}F-(*R*,*S*)-FIPCT have faster binding kinetics than ^{18}F-FECNT, with ^{18}F-FCT reaching maximal binding at 20 min (*14*) and ^{18}F-(*R*,*S*)-FIPCT reaching maximal binding at 75 min after injection in rhesus monkeys (*16*); however, as discussed above, these molecules also have SCRs that are among the lowest of those reported. Though not the shortest, the relatively short time to peak cerebral activity for ^{18}F-FECNT has proven useful for experiments that require multiple injections (scans) in 1 d (*24*).

Results from the 5 PD patients support the potential of ^{18}F-FECNT to define the existence and quantify the extent of abnormalities related to neurodegeneration within the striatal dopaminergic system. Figure 5A shows that an H&Y stage 1.5 subject still has a fairly intact dopamine system in the caudate nuclei, especially the left caudate and the left anterior putamen (caudate nucleus $>$ anterior putamen $\gg$ posterior putamen). This is to be expected in an early PD patient (*33*). In an H&Y stage 4 subject (Fig. 5B), the caudate nucleus shows much higher uptake than the putamen, but somewhat less uptake than the caudate nucleus of an H&Y stage 1.5 subject, and there is not much, if any, of a differential between the anterior and posterior putamen. This is not surprising in that PD has been reported to typically affect the posterior putamen first, followed by the anterior putamen, and affects the caudate nucleus last and the least (*33*). It has been reported that the caudate nucleus retains up to of 50% of its dopaminergic input even late in the course of the disease (*33*). The H&Y stage 4 subjects' left and right putamen-to-cerebellum ratios for ^{18}F-FECNT are far lower than the ratios of the H&Y stage 1.5 subjects and actually have virtually equal ^{18}F-FECNT uptakes, as shown in Figure 6 and Table 4. This confirms the potential of this ligand to quantitatively assess the loss of presynaptic dopaminergic neurons. Figure 5A also shows an H&Y stage 1.5 subject with bilaterally, asymmetrically decreased caudate and putamen uptake (with uptake in the left striatum being greater than uptake in the right striatum), despite the fact that on examination the subject was hemi-PD, having no complaints of PD and showing no signs of PD on the right side of her body. We saw the same pattern in our other H&Y stage 1.5, hemi-PD patient (Table 4). This supports

TABLE 4
Tissue-to-Cerebellum Ratios Compared with H&Y Scores of 5 PD Patients at 90 Minutes

Subject no.	Sex	H&Y score	Worst affected side	Ratio			
				R Caud:cer	R Put:cer	L Caud:cer	L Put:cer
1	F	1.5	L	4.5	2.7	6.4	3.4
2	M	1.5	R	6.2	2.9	5.4	2.5
3	F	2.5	L	4.0	2.0	4.7	1.9
4	F	4	Equal	3.7	1.8	3.9	1.8
5	M	4	L or equal	3.1	1.7	3.9	1.8

Caud = caudate nucleus; cer = cerebellum; Put = putamen.

the possible use of ^{18}F-FECNT PET imaging to detect PD presymptomatically although, clearly, more extensive ^{18}F-FECNT imaging studies are needed to test the feasibility of presymptomatic detection with this ligand.

CONCLUSION

^{18}F-FECNT has characteristics that make it an excellent fluorinated ^{18}F PET ligand for imaging DAT in the human brain. We are further exploring ^{18}F-FECNT's usefulness in the investigation of PD and related disorders as well as in assessing age-related effects on the central nervous system. We are hopeful that ^{18}F-FECNT indeed has the ability to detect presymptomatic PD on the apparently unaffected side of hemi-PD patients. Experiments to determine the correlation between ^{18}F-FECNT uptake and the H&Y scale and to the various subscores of the Unified Parkinson's Disease Rating Scale (*34*) are underway. ^{18}F-FECNT should have major advantages over conventional F-DOPA scanning for studying patients with advanced PD because it can be performed without restricting PD medications, there is no need to pretreat with carbidopa, and the study can be completed in $<$2 h. In summary, ^{18}F-FECNT represents an important new PET imaging ligand to assist in the investigation of dopamine-related disorders.

ACKNOWLEDGMENTS

The authors thank Drs. Ray L. Watts and Timothy Hanes for their assistance with this study. They also thank Kim Egeler, Margie Jones, Delicia Votaw, and Michael White for their technical assistance in acquisition and reconstruction of the PET scans.

REFERENCES

1. Pristupa ZB, Wilson JM, Hoffman BJ, Kish SJ, Nisnik HB. Pharmacological heterogeneity of the cloned and native human dopamine transporter: disassociation of [^{3}H]WIN 35,428 and [^{3}H]GBR 12,935 binding. *Mol Pharmacol.* 1994; 45:125–135.
2. Scheffel U, Dannals RF, Wong DF, Yokoi F, Carroll FI, Kuhar MJ. Dopamine transporter imaging with novel, selective cocaine analogs. *Neuroreport.* 1992;3: 969–972.
3. Kuikka JT, Bergstrom KA, Vanninen E, Laulumaa V, Hartikainen P, Lansimies E. Initial experience with single-photon emission tomography using iodine-123-labelled 2 beta-carbomethoxy-3 beta-(4-iodophenyl) tropane in human brain. *Eur J Nucl Med.* 1993;20:783–786.
4. Laruelle M, Wallace E, Seibyl JP, et al. Graphical, kinetic, and equilibrium analyses of in vivo [^{123}I]beta-CIT binding to dopamine transporters in healthy human subjects. *J Cereb Blood Flow Metab.* 1994;14:982–994.
5. Seibyl JP, Laruelle M, van Dyke CH, et al. Reproducibility of iodine-123-beta-CIT SPECT brain measurement of dopamine transporters. *J Nucl Med.* 1996;37: 222–228.
6. Innis RB, Seibyl JP, Scanley BE, et al. Single photon emission computed tomographic imaging demonstrates loss of striatal dopamine transporters in Parkinson disease. *Proc Natl Acad Sci USA.* 1993;90:11965–11969.
7. Seibyl JP, Marek KL, Quinlan D, et al. Decreased single-photon computed tomographic [^{123}I]beta-CIT striatal uptake correlates with symptom severity in Parkinson's disease. *Ann Neurol.* 1995;38:589–598.
8. Seibyl JP, Marek K, Sheff K, et al. Test/retest reproducibility of iodine-123-betaCIT SPECT brain measurement of dopamine transporters in Parkinson's patients. *J Nucl Med.* 1997;38:1453–1459.
9. Marek KL, Seibyl JP, Zoghbi SS, et al. [^{123}I] Beta-CIT/SPECT imaging demonstrates bilateral loss of dopamine transporters in hemi-Parkinson's disease. *Neurology.* 1996;46:231–237.
10. Ito Y, Fujita M, Shimada S, et al. Comparison between the decrease of dopamine transporter and that of L-DOPA uptake for detection of early to advanced stage of Parkinson's disease in animal models. *Synapse.* 1999;31:178–185.
11. Kazumata K, Dhawan V, Chaly T, et al. Dopamine transporter imaging with fluorine-18-FPCIT and PET. *J Nucl Med.* 1998;39:1521–1530.
12. Laakso A, Bergman J, Haaparanta M, Vilkman H, Solin O, Hietala J. [^{18}F]CFT [(^{18}F)WIN 35,428], a radioligand to study the dopamine transporter with PET: characterization in human subjects. *Synapse.* 1998;28:244–250.
13. Goodman MM, Keil R, Shoup TM, et al. Fluorine-18-FPCT: a PET radiotracer for imaging dopamine transporters. *J Nucl Med.* 1997;38:119–126.
14. Mach RH, Nader MA, Ehrenkaufer RL, et al. Fluorine-18-labeled tropane analogs for PET imaging studies of the dopamine transporter. *Synapse.* 2000;37: 109–117.
15. Wilson AA, DaSilva JN, Houle S. In vivo evaluation of [^{11}C]- and [^{18}F]-labelled cocaine analogues as potential dopamine transporter ligands for positron emission tomography. *Nucl Med Biol.* 1996;23:141–146.
16. Xing D, Chen P, Keil R, et al. Synthesis, biodistribution, and primate imaging of fluorine-18 labeled 2beta-carbo-1′-fluoro-2-propoxy-3beta (4-chlorophenyl)tropanes: ligands for the imaging of dopamine transporters by positron emission tomography. *J Med Chem.* 2000;43:639–648.
17. Chaly T Jr, Matacchieri R, Dahl R, Dhawan V, Eidelberg D. Radiosynthesis of [^{18}F] N-3-fluoropropyl-2-beta-carbomethoxy-3-beta (4′ methylphenyl) nortropane (FPCMT). *Appl Radiat Isot.* 1999;51:299–305.
18. Goodman MM, Kilts CD, Keil R, et al. ^{18}F-labeled FECNT: a selective radioligand for PET imaging of dopamine transporters. *Nucl Med Biol.* 2000;27:1–12.
19. Deterding TA, Votaw JR, Wang CK, et al. Biodistribution and radiation dosimetry of the dopamine transporter ligand. *J Nucl Med.* 2001;42:376–381.
20. Howell LL, Wilcox KM. The dopamine transporter and cocaine medication development: drug self-administration in nonhuman primates. *J Pharmacol Exp Ther.* 2001;298:1–6.
21. Volkow ND, Gatley SJ, Fowler JS, et al. Cocaine doses equivalent to those abused by humans occupy most of the dopamine transporters. *Synapse.* 1996;24: 399–402.
22. Volkow ND, Wang GJ, Fischman MW, et al. Relationship between subjective effects of cocaine and dopamine transporter occupancy. *Nature.* 1997;386:827–830.
23. Wilcox KM, Lindsey KP, Votaw JR, et al. Self-administration of cocaine and the cocaine analog RTI-113: relationship to dopamine transporter occupancy determined by PET neuroimaging in rhesus monkeys. *Synapse.* 2002;43:78–85.
24. Votaw JR, Howell LL, Martarello L, et al. Measurement of dopamine transporter occupancy for multiple injections of cocaine using a single injection of [F-18]FECNT. *Synapse.* 2002;44:203–210.
25. Hoehn MM, Yahr MD. Parkinsonism: onset, progression and mortality. *Neurology.* 1967;17:427–442.
26. Ahlskog JE, Uitti RJ, O'Conner MK, et al. The effect of dopamine agonist therapy on dopamine transporter imaging in Parkinson's disease. *Mov Disord.* 1999;14:940–946.
27. Innis RB, Marek KL, Sheff K, et al. Effect of treatment with L-dopa/carbidopa or L-selegiline on striatal dopamine transporter SPECT imaging with [^{123}I]beta-CIT. *Mov Disord.* 1999;14:436–442.
28. Nurmi E, Bergman J, Eskola O, et al. Reproducibility and effect of levodopa on dopamine transporter function measurements: a [^{18}F]CFT PET study. *J Cereb Blood Flow Metab.* 2000;20:1604–1609.
29. Wienhard K, Eriksson L, Grootoonk S, Casey M, Pietrzyk U, Heiss WD. Performance evaluation of the positron scanner ECAT EXACT. *J Comput Assist Tomogr.* 1992;16:804–813.
30. Lin KP, Huang SC, Yu DC, Melega W, Barrio JR, Phelps ME. Automated image registration for FDOPA PET studies. *Phys Med Biol.* 1996;41:2775–2788.
31. Staley JK, Basile M, Flynn DD, Mash DC. Visualizing dopamine and serotonin transporters in the human brain with the potent cocaine analogue [^{125}I]RTI-55: in vivo binding and autoradiographic characterization. *J Neurochem.* 1994;62:549–556.
32. Stout D, Petric A, Satyamurthy N, et al. 2Beta-carbomethoxy-3beta-(4- and 2-[^{18}F]fluoromethylphenyl)tropanes: specific probes for in vivo quantification of central dopamine transporter sites. *Nucl Med Biol.* 1999;26:897–903.
33. Rinne JO, Ruottinen H, Bergman J, Haaparanta M, Sonninen P, Solin O. Usefulness of a dopamine transporter PET ligand [^{18}F]beta-CFT in assessing disability in Parkinson's disease. *J Neurol Neurosurg Psychiatry.* 1999;67:737–741.
34. Fahn S, Elton RL, Members of the UPDRS Development Committee: Unified Parkinson's disease rating scale. In: Fahn S, Marsden CD, Goldstein M, Calne DB, eds. *Recent Developments in Parkinson's Disease*. 2nd ed. New York, NY: Macmillan; 1987:153–163.